

Processing challenges in the XMM-Newton slew survey

Richard D. Saxton^a, Bruno Altieri^a, Andrew M. Read^b, Michael J. Freyberg^c, M. Pilar Esquej^a
and Diego Bermejo^a

^aXMM-SOC, ESAC, Villafranca del Castillo, Apartado 50727, 28080 Madrid, Spain;

^bDepartment of Physics and Astronomy, University of Leicester, Leicester Le17RH, England;

^cMax-Planck-Institut fuer Extraterrestrische Physik, PO Box 1312, 85741 Garching, Germany.

ABSTRACT

The great collecting area of the mirrors coupled with the high quantum efficiency of the EPIC detectors have made XMM-Newton the most sensitive X-ray observatory flown to date. This is particularly evident during slew exposures which, while giving only 15 seconds of on-source time, actually constitute a 2-10 keV survey ten times deeper than current "all-sky" catalogues. Here we report on progress towards making a catalogue of slew detections constructed from the full, 0.2-12 keV energy band and discuss the challenges associated with processing the slew data. The fast (90 degrees per hour) slew speed results in images which are smeared, by different amounts depending on the readout mode, effectively changing the form of the point spread function. The extremely low background in slew images changes the optimum source searching criteria such that searching a single image using the full energy band is seen to be more sensitive than splitting the data into discrete energy bands. False detections due to optical loading by bright stars, the wings of the PSF in very bright sources and single-frame detector flashes are considered and techniques for identifying and removing these spurious sources from the final catalogue are outlined. Finally, the attitude reconstruction of the satellite during the slewing manoeuvre is complex. We discuss the implications of this on the positional accuracy of the catalogue.

Keywords: XMM-Newton, X-rays, sky surveys, data analysis, slew

1. INTRODUCTION

XMM-Newton¹ performs slewing manoeuvres between observation targets with the EPIC cameras open and the other instruments closed. Both EPIC-pn² and EPIC-MOS³ are operated during slews with the Medium filter in place and the observing mode set to that of the previous observation.

The satellite moves between targets by performing an open-loop slew along the roll and pitch axes and a closed-loop slew, where measurements from the star tracker are used in addition to the Sun-sensor measurements to provide a controlled slew about all three axes, to correct for residual errors in the long open-loop phase. The open-loop slew is performed at a steady rate of about 90 degrees per hour and it is data from this phase which may be used to give a uniform survey of the X-ray sky.

Slew Data Files (SDF) have been stored in the XMM-Newton Science Archive (XSA) from revolution 314 and there are currently 465 SDFs stored with a mean slew length of 86 degrees (Fig. 1). Not all of these data are scientifically useful and the sky coverage will be discussed in Sect. 2.

The data are being used to perform three independent surveys, a soft band (0.2-2 keV) X-ray survey with strong parallels to the ROSAT all-sky survey⁴(RASS), a hard band (2-12 keV) survey and an XMM-Newton full-band (0.2-12 keV) survey.

Theoretically the good point spread function of the X-ray telescopes⁵ should allow source positions to be determined to an accuracy of better than 6 arcseconds, similar to that found for faint objects in the 1XMM catalogue of serendipitous sources detected in pointed observations (*). Any errors in the attitude reconstruction for the slew could seriously degrade this performance and a major technical challenge of the data processing is to achieve the nominal accuracy. We address this issue in Sect. 4.

Further author information: (Send correspondence to R.D.S.)

R.D.S.: E-mail: Richard.Saxton@sciops.esa.int, Telephone: +34 91 8131306

B.A.: E-mail: Bruno.Altieri@sciops.esa.int, Telephone: +34 91 8131340

*The First XMM-Newton Serendipitous Source Catalogue, XMM-Newton Survey Science Centre (SSC), 2003.

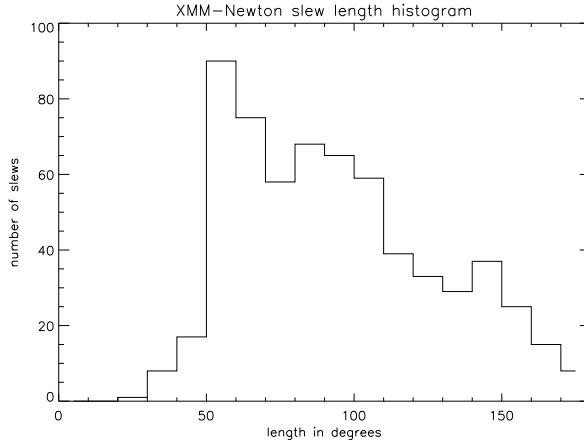


Figure 1. A histogram of the distance across the sky covered by individual slews.

2. OBSERVATIONS AND DATA ANALYSIS

The appearance of a source in the slew depends on the frame time of the observing mode as photons can only be positioned in space to an accuracy of one frame. This has major implications for MOS, where the relatively long frame time of 2.6 seconds, spreads out a source into a 4 arcminute long streak (Fig. 2). EPIC-pn has a much faster readout and source extension in the slew direction is less than 18 arcseconds in all observing modes. The relatively large source profile in the MOS cameras and their lower effective area make the EPIC-pn a much superior instrument for performing a slew survey. For this reason only pn data are being used in the data analysis.

Sources pass through the field of view of EPIC-pn in about 15 seconds. This low exposure time leads to a generally very low background of average $0.1 \text{ c/arcminute}^2$ in normal conditions. However, some slews taken at times of enhanced solar activity do exhibit higher background (Fig. 3) and can give rise to a large number of spurious sources. For each slew we have computed average band rates in 6 energy bands to characterize the general rate level. In this first processing slews with high background that had an average count rate exceeding 5.5 c/s in the $7.5 - 12 \text{ keV}$ band are being discarded. In later processings we will also use low-background periods of contaminated slews using time selections, which will yield another $\sim 10\%$ exposure time.

A total of 605 slew datasets have been processed and stored in the XSA. Of these 424 have been made with pn in the useful FF (295), eFF (88) and LW (41) modes respectively. After removal of the high background slews we are left with 312 slews, with a mean sky area of the useable part of the data of ~ 25 square degrees, giving a total sky coverage of some 8,000 square degrees, ignoring overlaps. The sky coverage is uniform but subject to the vignetting function such that sources passing directly through the centre of the detector receive an equivalent of 11 seconds of on-axis exposure while sources further from the centre receive less. The mean equivalent on-axis exposure time over the sky is 6.3 seconds and the sky area covered as a function of exposure time is shown in Figure 4.

Events are recorded initially in RAW or detector coordinates and have to be transformed, using the satellite attitude history, into sky coordinates. The tangential plane geometry commonly used to define a coordinate grid for flat images is only valid for distances of 1–2 degrees from a reference position, usually placed at the centre of the image. To avoid this limitation, slew datasets are divided into roughly one square degree event files, attitude corrected and then converted into images. This relies on the attitude history of the satellite being accurately known during the slew; a point which is addressed in section 4.

2.1. Instrumental aspects

The XMM-Newton Slew Data Files (SDFs) for EPIC-pn were processed using the `epchain` package of the public `xmmsas-6.1` plus a small modification for the `oal` library. For diagnostic reasons a few parameters were set to

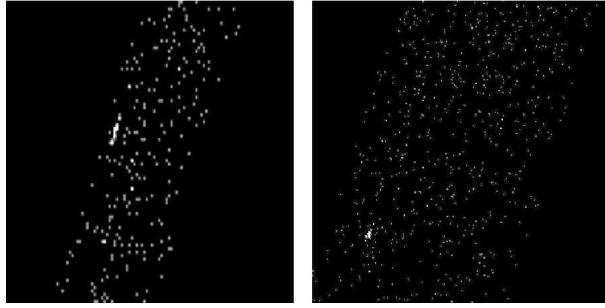


Figure 2. The appearance of a source in a MOS (left) and EPIC-pn (right) slew image. Note the extension in the slew travel direction in the MOS image due to integration over a frame time of 2.6s.

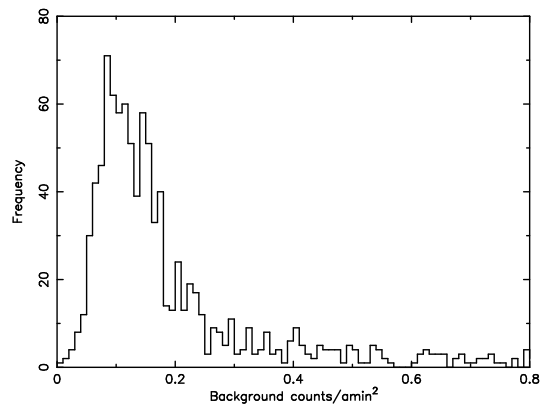


Figure 3. A histogram of the total band (0.2-12 keV) EPIC-pn background levels in units of counts/arcminute².

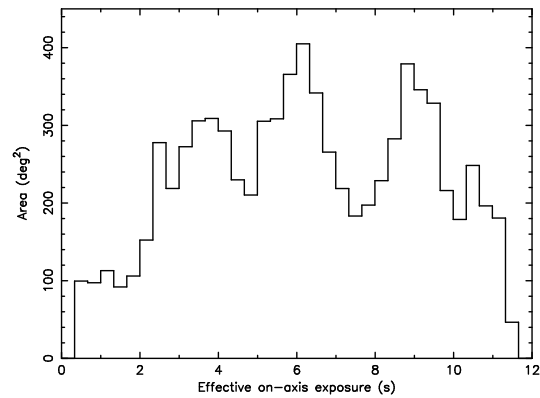


Figure 4. A histogram of the total band (0.2-12 keV) EPIC-pn sky coverage as a function of effective on-axis exposure time. The histogram has been normalised to a total of 8,000 square degrees.

non-default values (e.g., keeping also events below 150 eV).

For the *Slew Survey* catalogue we selected only EPIC-pn exposures performed in *Full Frame* (FF), *Extended Full Frame* (eFF), and *Large Window* (LW) modes, i.e. modes where all 12 CCDs are integrating (in LW mode only half of each CCD). The corresponding cycle times are 73.36 ms, 199.19 ms, and 47.66 ms, which converts to a scanned distance of 6.6 arcseconds, 17.9 arcseconds, and 4.3 arcseconds per cycle time, respectively. In the *Small Window* mode only the central CCD is operated and a window of 64×64 pixels is read out, i.e. only about 1/3 of a CCD. In the fast modes, *Timing* and *Burst*, only 1-dimensional spatial information for the central CCD is available and thus these modes are not very well suited for source detection. Therefore for these three modes the *Closed* filter position will be used in the future instead of the *Medium* position, to utilize this unusable exposure time for calibration purposes.

2.2. Source search procedure

Pilot studies were performed to investigate the optimum processing and source-search strategies. By making small changes to the XMM-*Newton* standard analysis software (SAS) we have been able to successfully create and use correct exposure maps in the source searching. These produced no unusual effects, although uneven (and heightened) slew exposure is observed at the end of slews (the 'closed-loop' phase). We tested a number of source-searching techniques and found that the optimum source-searching strategy was usage of a semi-standard 'eboxdetect (local) + esplinemap + eboxdetect (map) + emldetect' method, tuned to \sim zero background, and performed on a single image containing just the single events (pattern=0) in the 0.2–0.5 keV band, plus single and double events (pattern=0–4) in the 0.5–12.0 keV band. This is similar to the technique used for producing the RASS catalogue⁶ and resulted in the largest numbers of detected sources, whilst minimising the number of spurious sources due to detector anomalies (usually caused by non-single, very soft (<0.5 keV) events). The source density was found to be \approx 0.5 sources per square degree to an emldetect detection likelihood threshold (DET_ML) of 10 (approx 3.9σ).

In the current and on-going slew pipeline, images and exposure maps have been created and source-searched. This is being done in 3 separate energy bands: full band (0.2–0.5 keV [pattern=0] + 0.5–12.0 keV [pattern=0–4]), soft band (0.2–0.5 keV [pattern=0] + 0.5–2.0 keV [pattern=0–4]), and hard band (2.0–12.0 keV [pattern=0–4]). In this processing we are now recording detections down to an *emldetect* detection likelihood threshold of 8 (approx 3.4σ), and detecting \approx 0.7 sources per square degree.

3. SPURIOUS SOURCES

Systematic effects exist with the instrument and detection software which lead to a number of spurious detections. The three principle causes are outlined below.

3.1. Optical loading

EPIC-pn slew exposures are possibly affected by optical loading contamination. This effect is due to several optical photons (each creating a 3.65 eV charge) piling-up above the low-energy threshold of 20 ADUs and creating fake X-ray counts. On pointed observation this effect is removed by offset maps acquired at the start of each exposure and subtracted on-board, but this is not the case for slew exposures, where the offset map of the previous (pointed) exposure is applied. As a consequence, very bright stars could be affected by optical loading in the XMM slew survey.

Based on the measured optical transmission of the Medium filter and theoretical considerations, optical loading is expected for stars brighter than magnitude $V=3.7$, where more than 5 counts would be due optical photons.

The optical loading has been assessed using bright USNO stars detected in the slew survey. Figure 5 shows soft band slew counts plotted against their R magnitude. Stars fainter than $R=4$ are not affected by optical loading, as no correlation is found between their count rate and magnitude. Stars brighter than $R=4$ could possibly be affected by optical loading counts although it is not yet clear to what extent. Some evidence shows that it would play only a minor role for stars down to $R=2$. Two $V=2.7$ stars have been detected so far with less than 10 counts, much less than expected from optical loading only, so optical loading might not be an issue at all.

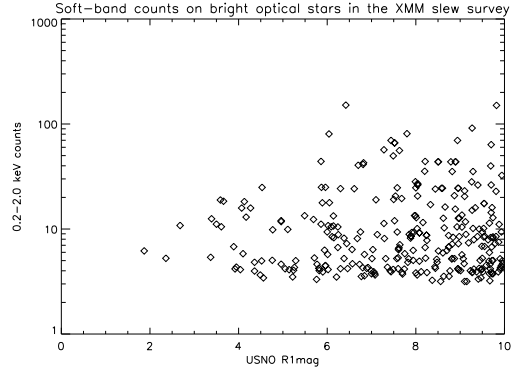


Figure 5. A plot of counts detected in the soft band against R magnitude for counterparts taken from the USNO catalogue.

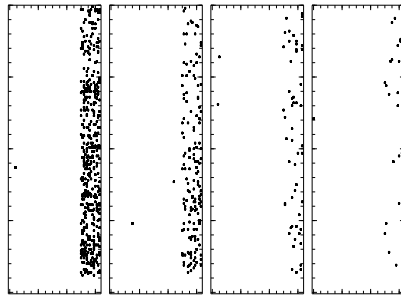


Figure 6. Four consecutive EPIC-pn frames showing a large number of (low-energy) events distributed along neighbouring columns; these features can easily be discriminated from astronomical sources in detector and time space (but are more difficult to distinguish once projected onto the sky).

3.2. Detector flashes

We have created lightcurves with short time bin size (< 1 s) in the softest channels to identify short-duration CCD flashes that occur only for < 200 ms in several adjacent CCD columns with a very soft spectrum. Projected onto the sky these can lead to spurious sources. Figure 6 shows 4 consecutive readout frames containing one of these flashes.

These effects are minimised by only using single-pixel (pattern 0) events for photon energies less than 500 eV. Nevertheless, some flashes may be manifest in slew images and so sanity checks of data and detector performance are made on the basis of diagnostic images and lightcurves of each individual CCD.

3.3. The wings of very bright sources

It was noticed in the creation of the 1XMM serendipitous source catalogue that, due to the imperfect modelling of the PSF, a halo of false detections is often seen around bright sources. The same effect is seen in slew exposures but due to the reduced exposure time is only important for very bright sources $\gg 10$ c/s. In addition large extended sources often result in multiple detections of the same object. It is fairly easy to identify occurrences by searching for images with a large number of sources. A histogram of source counts (Fig. 7) shows several outliers from the main distribution including one image containing 46 sources; which is actually due to Puppis-A (see Fig 15).

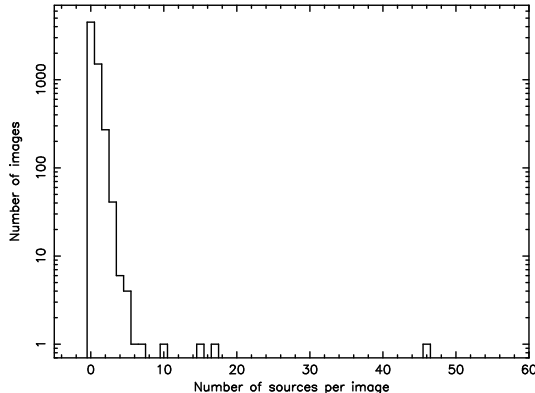


Figure 7. A histogram of the number of sources found in a single one degree image.

4. ATTITUDE RECONSTRUCTION AND POSITIONAL ACCURACY

This section describes the issue of attitude reconstruction in slew observations, which is crucial in the determination of source coordinates. After showing how the attitude reconstruction is generally performed, we will concentrate on that of the open-loop slews which have been used in this survey.

The attitude information of the XMM-Newton satellite is provided by the Attitude and Orbit Control Subsystem (AOCS). A star tracker co-aligned with the telescopes allows up to a maximum of five stars to be continuously tracked giving accurate star position data every 0.5 seconds, which operates in addition to the Sun sensor that provides a precise Sun-line determination. Such information is processed resulting in an absolute accuracy of the reconstructed astrometry of typically 1 arcsecond. For the open-loop slews, large slews outside the star-tracker field of view of 3 x 4 degrees, the on-board software generates a three axis momentum reference profile and a two-axis (roll and pitch) Sun-sensor profile, both based on the ground slew telecommanding. During slew manoeuvring a momentum correction is superimposed onto the reference momentum profile and, as there are no absolute measurements for the yaw axis, a residual yaw attitude error exists at the end of each slew that may be corrected in the final closed-loop slew.

So far, two types of attitude data can be used as the primary source of spacecraft positioning during event files processing. They are the Raw Attitude File (RAF) and the Attitude History File (AHF). For pointed observations, the RAF provides the attitude information at the maximum possible rate, with one entry every 0.5 seconds while the AHF is a smoothed and filtered version of the RAF, with times rounded to the nearest second. In slew datasets the RAF stores attitude information every 40–60 seconds while the AHF contains identical positions with timing information in integer seconds. The user can select which one to use for data processing by setting an environment variable.

In a pilot study where the AHF was used for attitude reconstruction, source detection was performed and their correlations with ROSAT and 2MASS catalogues indicated a slew relative pointing accuracy of ~ 10 arcseconds, enough for a good optical follow up of the sources. However, an absolute accuracy of 0-60 arcseconds (30 arcsecond mean) was obtained in the slew direction, resulting in a thin, slew-oriented error ellipse around each source. This error appears to be consistent with the error introduced by the quantisation of the time to 1 second in the attitude file and leads us to change the processing software as a better accuracy should be obtained. Investigating further the errors, the RAF was used to compute the astrometry for some observations as a test. In this case, an offset of ~ 1 arcminute from the ROSAT positions was found, but with a smaller scatter compared with the positions returned by the AHF processing. The consistency of these offsets suggested that they could be due to a timing issue. This has been confirmed by flight dynamics who stated that the tracking of up to five stars, mentioned above, produces a delay from the CCD exposure to data availability of approximately 0.75 seconds. Subtracting directly this 0.75 seconds from every entry in the RAF we obtain an optimal attitude file for the processing.

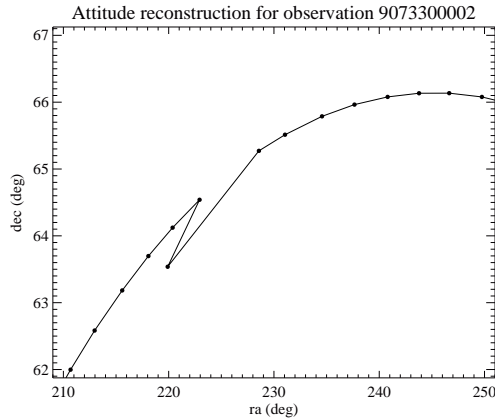


Figure 8. A zoom into the problematic region of the attitude file in the slew 9073300002 before removing the bad RAF point. The points show the generated attitude information and the line shows the interpolation between the points. After the correction such a line becomes smooth.

Other issues affecting the astrometry performance appeared after a careful visual examination of the RAF files, where two types of peculiarities appeared in some of the slews both affecting a localised region or the totality of the slew. This means that if a source lies in a problematic region its position has not been correctly generated. On the one hand, 5 observations presented sharp discontinuities revealing the existence of single bad RAF points that have to be determined and removed from the attitude file before performing the source searching. As an example a source in the slew 9073300002 was discovered to have a closest ROSAT counterpart at a distance of 8 arcminutes. Investigation showed that the source was observed at a time coincident with a large error in the attitude file (Fig. 8). After the bad RAF point was removed the recalculated source position lies at 11 arcseconds from the ROSAT position. On the other hand the attitude reconstruction of some slews appeared not smooth but turbulent in 7 observations (Fig. 9) and this case is still under investigation.

Slew observations have been reprocessed using corrected RAFs and a subsample of 1260 non-extended sources (defined as having an extent parameter < 2 from the emldetect source fitting) with $DET_ML > 10$, have been correlated with several catalogues within a 60 arcsecond offset. The correlation with the RASS reveals that $\sim 60\%$ of the slew sources have an X-ray counterpart of which 68% (90%) lie within 16 (31) arcseconds (Fig. 10). This gives confidence that the majority of slews have well reconstructed attitude. Tests on some of the outliers show that closer matches are sometimes available using ROSAT pointed data from the 2RXP and 1RXH catalogues. To form a sample of catalogues with highly accurate positions but which minimise the number of false matches, we used the Astrophysical Virtual Observatory (AVO) to correlate the slew positions against non-X ray SIMBAD catalogues. This gave 508 matches of which 68% (90%) were contained within 8 (17) arcseconds (Fig. 11), showing that the positional accuracy of the slew is not much worse than the observed limit for low significance XMM-*Newton* sources.

5. RESULTS

To date 138 datasets have been processed giving 2370 sources with $DET_ML > 8$ (1600 with $DET_ML > 10$) in the total band and 440 in the hard X-ray band (220 with $DET_ML > 10$). A small pilot study visualising all $DET_ML > 10$ sources from ten slews, showed that apart from the problems detailed in section 3, sources appeared to be real. More sophisticated statistical tests or simulations will have to be applied to calculate the fraction of sources with DET_ML between 8 and 10 which are due to background fluctuations.

A great variety of sources have been detected, including stars, galaxies, both interacting and normal, AGN, clusters of galaxies and SNR plus extremely bright Low-Mass-X-ray Binaries (LMXB), with several hundred c/s.

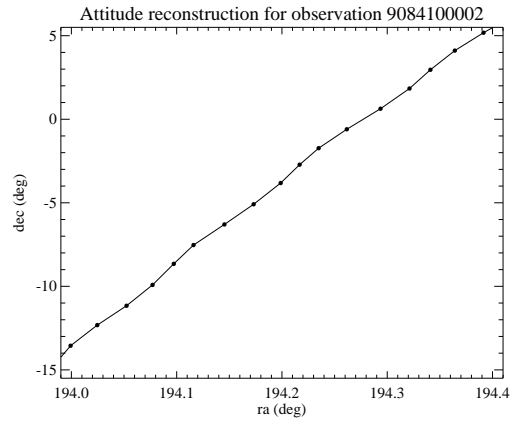


Figure 9. A plot showing non-smooth, or turbulent, attitude reconstruction in the revolution 0841 attitude file.

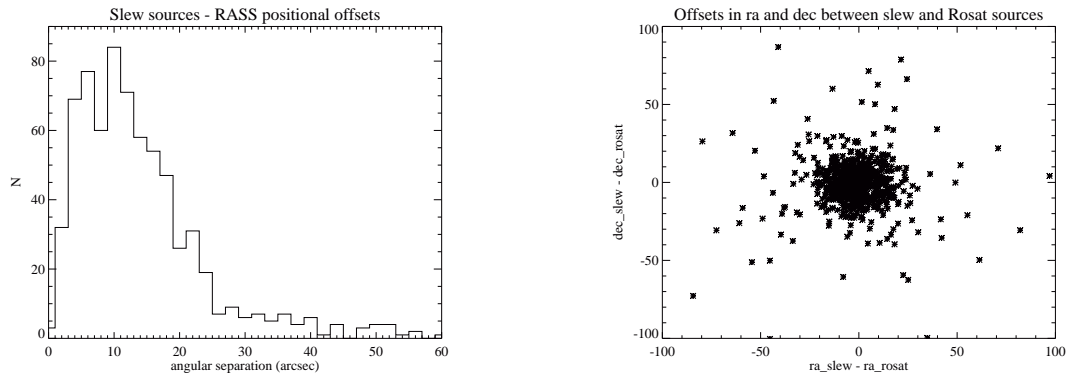


Figure 10. A comparison of slew source positions with those from the RASS catalogue. 68% of the sources lie within 16 arcseconds. The left panel shows a histogram of the offset magnitude while the right panel gives the absolute offset in ra and dec of the slew source from the ROSAT position.

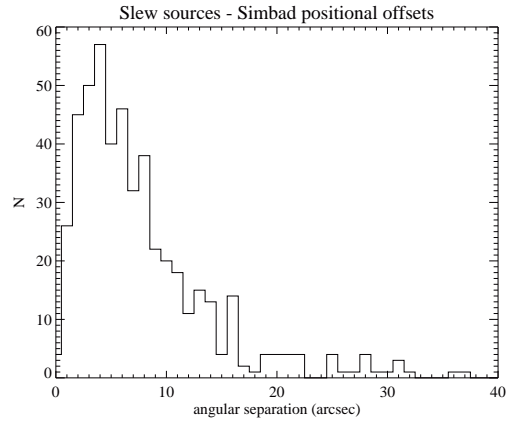


Figure 11. A histogram of the distribution of the angular separation in arcsecond derived from the correlation of the slew sources with the Simbad database within a 40 arcsecond offset. 68% of the matches lie within 8 arcseconds.

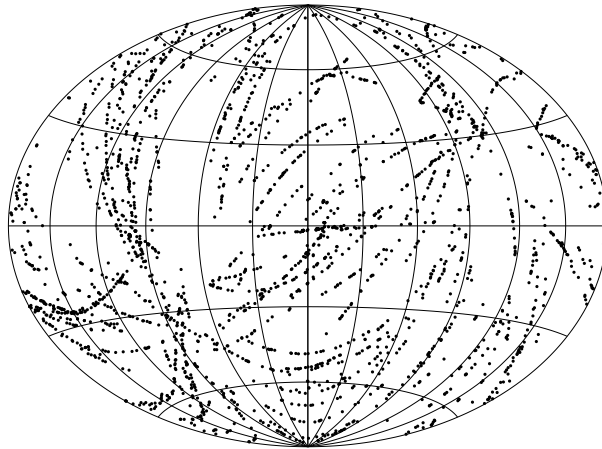


Figure 12. An Aitoff projection of the distribution of all slew sources on the sky in galactic coordinates.

These are bright enough to give a useful spectrum although they suffer seriously from photon pile-up. As we are essentially performing three separate surveys, we have immediate access to hardness ratios for many of the detected sources, and a large variation in source hardness is seen. About one percent of sources are detected in more than one slew, yielding short to medium term (days to months) variability information. One source, so far detected in three separate slews, appears to have varied in flux by a factor of ~ 2 .

Figure 12 shows the distribution of sources over the sky indicating the paths of slews processed so far. The flux limits for the three surveys are compared with those of other missions in Fig 13. At a DET_ML of 10(8) sources are detected to a flux limit of $6(4.5) \times 10^{-13} \text{ ergs s}^{-1} \text{ cm}^{-2}$ in the soft band and $4(3) \times 10^{-12} \text{ ergs s}^{-1} \text{ cm}^{-2}$ in the hard band. The mean flux limit over the whole survey, taking into account the variable effective on-axis exposure time, is 60% higher than these values.

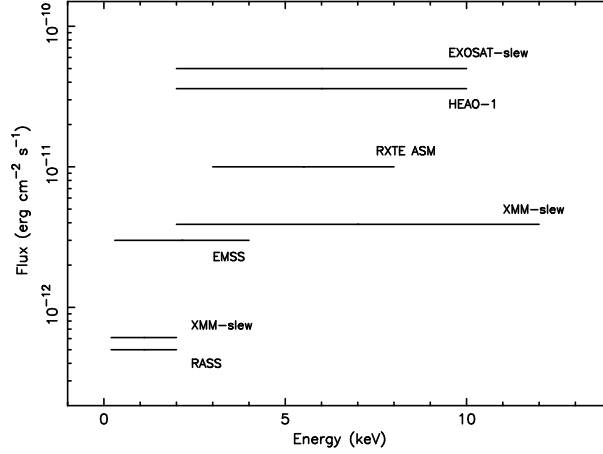


Figure 13. The flux limits of X-ray large area surveys. The XMM-*Newton* limits have been calculated for a DET_ML=10 source, with an absorbed power-law spectrum of slope 1.7 and $N_H=3.0 \times 10^{20} \text{ cm}^{-2}$, passing through the centre of the field of view.

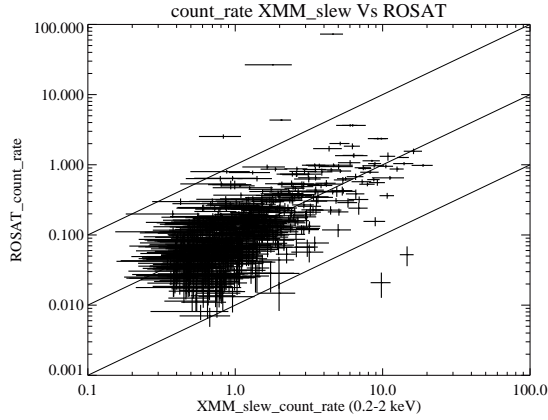


Figure 14. A comparison of the count rates in the XMM soft band and the RASS. The central line represents the mean ratio of ~ 10 and the outer lines variability by a factor of ten.

5.1. Global correlations with the ROSAT all-sky survey

There is a strong overlap between the soft XMM slew catalogue and the ROSAT all-sky survey (RASS) which is limited by statistics at the faint flux end of each survey and by intrinsic source variability. Of the non-extended, DET_ML > 10 sources in the soft band slew survey 64% have counterparts within 1 arcminute in the RASS. The fraction drops to 53% for hard band slew sources. A comparison of the two surveys reveals a mean count rate ratio of ~ 10 (Fig. 14), with one percent of the sources detected in both surveys showing variability by a factor in excess of 10. Many more variable sources will be identified by performing an upper limits analysis on data from both surveys. The combination of these surveys will enable the long term X-ray variability of several thousand sources to be studied over a baseline of 10–15 years. The high variability sources so far identified are formed from Blazars, low-mass X-ray binaries, eclipsing binaries and Seyfert I galaxies.

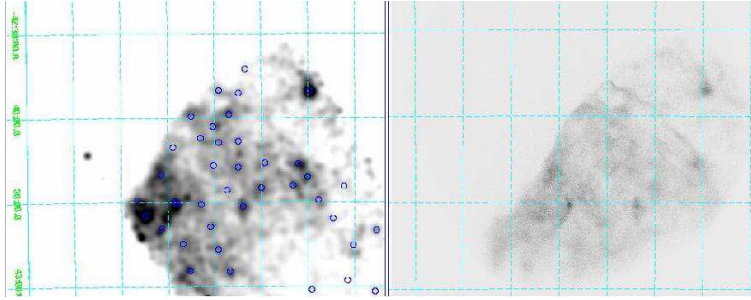


Figure 15. A comparison of an adaptively smoothed, exposure corrected, XMM slew image of the Puppis-A SNR (left) with a ROSAT-HRI, 7000 second pointed exposure, taken in 1992 (right). The XMM image is limited by the 0.5 degree width of the pn camera while the ROSAT image is cut by the bottom edge of the HRI detector. The small circles in the XMM image indicate the positions of detections made by the source search software.

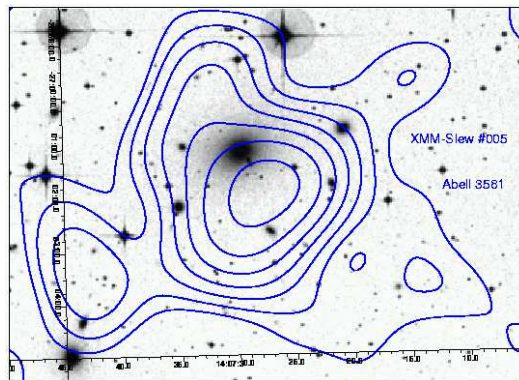


Figure 16. Contours of X-ray emission from a single slew across the galaxy cluster Abell 3581, superimposed on a DSS image.

5.2. Extended sources

The good spatial resolution and low background of XMM-*Newton* allows the slew survey to usefully image bright extended sources. The very bright, large, SNR PUPPIS-A was slewed over in 2002 and the X-ray emission shows structure in a smoothed image which correlates well with that seen in a pointed ROSAT HRI observation (Fig. 15). Nearby clusters of galaxies, such as Abell 3581, can also be clearly detected as extended (Fig. 16) and there is the possibility that at the faint end of the survey new clusters or galaxy groups, too small to be detected as extended in the RASS, will be discovered.

6. SUMMARY

The XMM-*Newton* slew data constitute a wide area (currently 20% of the sky) shallow survey whose soft band flux limits are sufficiently deep to provide an interesting comparison with the RASS and whose hard band limits represent an order of magnitude improvement over previous missions. Several technical challenges have been overcome, particularly in understanding and refining the astrometry and in rejecting spurious sources. The astrometry is good, with a 1 sigma position error of 8 arcseconds, easily sufficient to allow an optical follow-up of these high flux X-ray sources. Data processing is progressing well and the final total energy band catalogue should contain between three and five thousand sources, depending on the final choice of maximum likelihood detection threshold employed. The hard band catalogue will contain between 400 and 800 sources.

ACKNOWLEDGMENTS

This research has made use of the SIMBAD database, operated at CDS, Strasbourg, France. We thank the Astrophysical Virtual Observatory (AVO) for providing software tools. AVO has been awarded financial support by the European Commission through contract HPRI-CT-2001-50030 under the 5th Framework Programme for research, technological development and demonstration activities. Based on data obtained with XMM-Newton, an ESA science mission with instruments and contributions directly funded by ESA Member States and NASA. Congratulations are due to the designers and operators of the attitude control system for providing an accurate satellite pointing position throughout slewing manoeuvres. We thank Georg Lammers and Herman Brunner for providing source search software which proved to be robust on slew data. We also thank Mark Tuttlebee, Pedro Rodriguez, John Hoar and Aitor Ibarra for their help with understanding the slew attitude history files.

REFERENCES

1. F. Jansen, D. Lumb, B. Altieri, J. Clavel, M. Ehle, C. Erd, C. Gabriel, M. Guainazzi, P. Gondoin, R. Much, R. Munoz, M. Santos, N. Schartel, D. Texier, and G. Vacanti, “Xmm-newton observatory,” *A&A* **365**, pp. L1–6, 2001.
2. L. Struder, U. Briel, K. Dennerl, R. Hartmann, E. Kendziorra, N. Meidinger, E. Pfeffermann, C. Reppin, B. Aschenbach, W. Bornemann, *et al.*, “The european photon imaging camera on xmm-newton: The pn-ccd camera,” *A&A* **365**, pp. L18–26, 2001.
3. M. Turner, A. Abbey, M. Arnaud, M. Balasini, M. Barbera, E. Belsole, P. Bennie, J. Bernard, G. Bignami, M. Boer, *et al.*, “The european photon imaging camera on xmm-newton: The mos cameras,” *A&A* **365**, pp. L27–35, 2001.
4. W. Voges, B. Aschenbach, T. Boller, H. Braeuninger, W. Burkert, K. Dennerl, J. Englhauser, R. Gruber, F. Haberl, *et al.*, “The rosat all-sky survey bright source catalogue,” *A&A* **349**, pp. 389–405, 1999.
5. B. Aschenbach, U. Briel, F. Haberl, H. Braeuninger, W. Burkert, A. Andreas, P. Gondoin, and D. Lumb, “Imaging performance of the xmm-newton x-ray telescopes,” in *X-Ray Optics, Instruments, and Missions III*, J. Truemper and B. Aschenbach, eds., *Proc. SPIE* **4012**, pp. 731–739, 2000.
6. R. Cruddace, G. Hasinger, and J. Schmitt, “The application of a maximum likelihood analysis to detection of sources in the rosat data base,” in *Astronomy from Large Databases. Scientific objectives and methodological approaches*, F. Murtagh and A. Heck, eds., *ESO Conference and Workshop Proceedings*, pp. 177–182, 1988.